Development of a CW NCRF Photoinjector using Solid Freeform Fabrication

Final Report

Phase II Award # **DE-SC0000869**

Period of performance: 08/15/2010 – 07/01/2013

PI: Pedro Frigola

RadiaBeam Technologies, LLC
1717 Stewart St
Santa Monica, CA 90404

Table of Contents

A. Significance, Background, and Technical Approach

The development of very high duty cycle, high gradient photoinjectors is critical for the next generation of accelerator systems, such as X-ray free-electron lasers (FELs) [1], inverse Compton scattering (ICS) sources [2], energy recovery linacs (ERLs) [3,4,5,6], injectors for linear colliders [7], as well as a variety of industrial systems for homeland security applications [8]. NCRF photoinjectors have a proven track record at generating the high quality beams necessary for these applications, however they are limited in large part to relatively low duty cycles due to ohmic wall looses. Thus a key issue for high average power, normal conducting, photoinjectors is effective structure cooling [9]. The fabrication of current high average-power photoinjectors relies on conventional design and fabrication techniques with many limitations [9]. Advances in Solid Freeform Fabrication (SFF) technology may make it possible to design and produce near net-shape copper structures for the next generation of very high rep rate, high gradient radio frequency (RF) photoinjectors. RF and thermal-management optimized geometries could be fully realized without the usual constraints and compromises of conventional machining techniques*. Further advances in SFF and powder metallurgy (P/M) techniques, with the ability to fine tune material properties, may soon make it possible to produce monolithic, thermally robust RF structures faster and cheaper than ever before.

In this Final Report we summarize our Phase II results and progress towards the construction and testing of a Proof of Principle (PoP) CW, high brightness gun with re-entrant cavity, using SFF.

The use of re-entrant cavity design is an important step towards increasing the duty cycle of NCRF photoinjectors. It is well known that the re-entrant cavity design (see X) provides significant advantages over the traditional pillbox design, while preserving all the characteristics of high brightness photoinjector design [10]. Both the re-entrant and pillbox designs support high accelerating gradients at the cathode, and allow for the emittance compensation approach towards beam dynamics, the critical features to produce electron-beams having 1 nC charge per bunch and normalized emittances near $\varepsilon_n = 10^{-6}$ m-rad. However, a re-entrant cavity design maximizes the accelerating field for a given RF power density at the walls surface [11]. Nevertheless, even with the advantages of the re-entrant cavity, the problem of RF power dissipation catches up at CW operation mode, and further improvement to the injector's cooling efficiency are needed.

SFF technologies, such as ARCAM's Electron Beam Melting (EBM) employ so-called rapid prototyping layer methods to allow for virtually any geometry to be physically constructed. Rapid prototyping, or more generally Solid Freeform Fabrication, refers to a group of techniques used to quickly fabricate a part layer-by-layer using 3D computer aided design (CAD) data. These techniques are common today throughout industry, providing a quick and accurate way for designers and engineers to visualize, optimize, and fabricate parts directly from CAD models. However, until recently, these methods have been primarily used to produce parts made from

* RadiaBeam Patent US 7,411,361

either thermoplastics or special sintered (not fully-dense) metals. The direct metal freeform fabrication technique being explored in this proposal is similar to other rapid prototyping technologies in their approach to fabrication. However, Arcam's EBM SFF technique is unique in that they can produce fully-dense metal components with properties similar to or better than that of wrought materials [12, 13].

The advantages afforded by using Arcam's EBM SFF to manufacture RF photoinjectors are considerable. The addition of embedded, conformal cooling channels will be an immediate improvement to many current designs. Although some state-of-the-art photoinjectors currently use conformal cooling channels, notably the LCLS photoinjector [14], such features come at a very high price and complexity due to the numerous circuits and brazing cycles required to accomplish them using conventional machining techniques. In Figure 1, a rendering of a photoinjector gun is shown with shaped conformal cooling channels that are possible only with SFF. Such shaped, conformal, axysymmetric channels would result in greatly enhanced heat transfer and more uniform cooling (no hot spots). These are features that are possible only with SFF techniques.

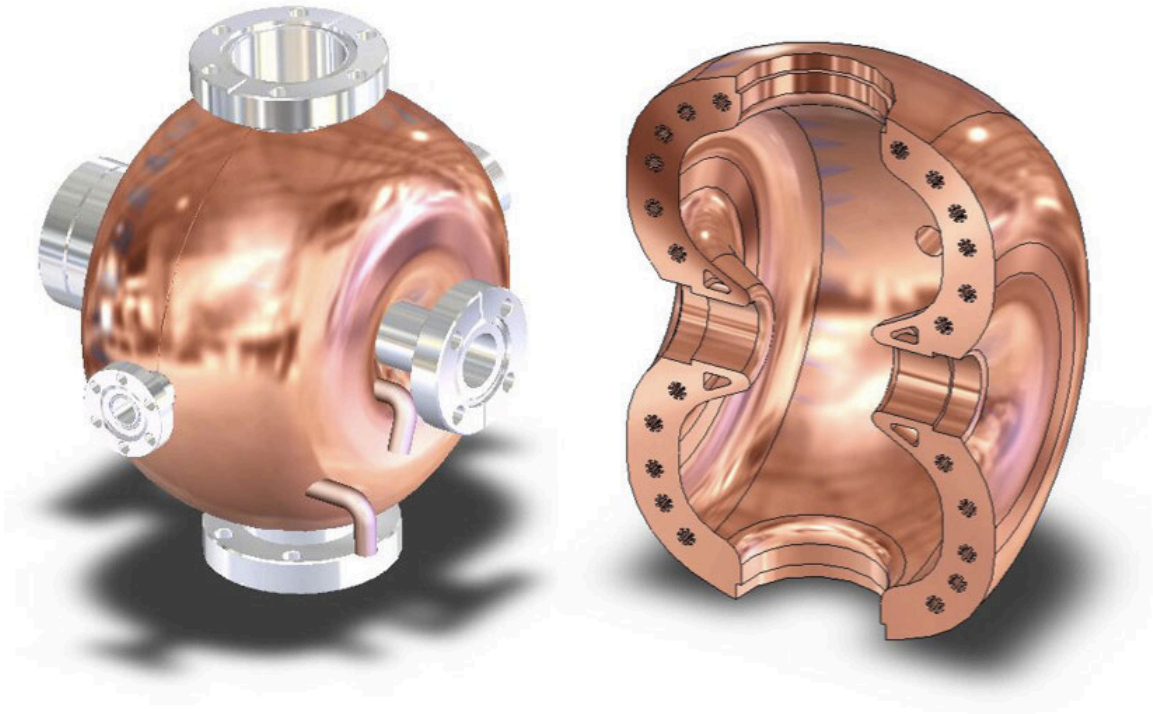

Figure 1: CAD rendering of the proposed SFF CW gun showing a final prototype assembly (Left), and a crossectional view of the copper cavities with shaped cooling channels (Right).

B. Phase II Results

The focus of the Phase II effort was the optimization of the Electron Beam Melting (EBM) additive manufacturing (AM) process for the production of the CW Gun geometry. We have successfully optimized EBM process parameters for pure copper, and to the extent possible in the current EBM machine, for the CW Gun geometry. RF testing was planned for, however, it was not carried out.

The bulk of this work resulted in the first EBM AM process optimization for pure copper, and has drawn significant interest from the EBM AM community. Oak Ridge National Laboratory's Manufacturing Demonstration Facility (ORNL-MDF), which utilizes the same EBM technology, contacted RadiaBeam Technologies and collaborators UTEP and NCSU, and expressed interested in using the copper themes developed to produce high efficiency heat exchangers in energy generation applications.

B.1. *Phase II Technical Objectives Compliance Matrix*

Technical Objective	Status	Comments
1. Finalize RF, thermal, and mechanical design.	Completed	RF design has been completed.
2. Optimize EBM process parameters and fabricate copper cells.	Completed	Samples were fabricated and successfully tested, a complete half cell structure was fabricated.
3. Assemble gun: secondary machining, joining, and ancillary components	Partially completed	Several prototypes cells were fabricated using EBM, however they contained material flaws.
4. Conduct cold test measurements, tuning, and high power testing	Partially completed	No RF testing was carried out. However, vacuum braze run, leak checks, and cooling circuit test was carried out.

B.2. *Finalize RF, thermal, and mechanical design*

B.2.1. RF Design

Considerable work was performed in Phase I, in collaboration with JLab, in the RF and thermal design of the SFF CW gun. In Phase II we largely focus on the design and integration of the RF coupler and ancillary gun components necessary for testing at JLab.

A Cooperative Research and Development Agreement (CRADA) was executed between RadiaBeam and JLab. A design review was held at JLab in January of 2011, and options for the coupler and ancillary components were addressed.

JLab will provide a 50 kW CW RF window and infrastructure for prototype testing. The high power window is matched at 1497 MHz in WR650 waveguide and can be used in a simple flange with o-rings as a gas barrier, guard vacuum seal, or in a conflat-style knife edge seal for UHV operation. JLab has optimized the window design, and has conducted RF power test varying it's performance (See Figure 2).

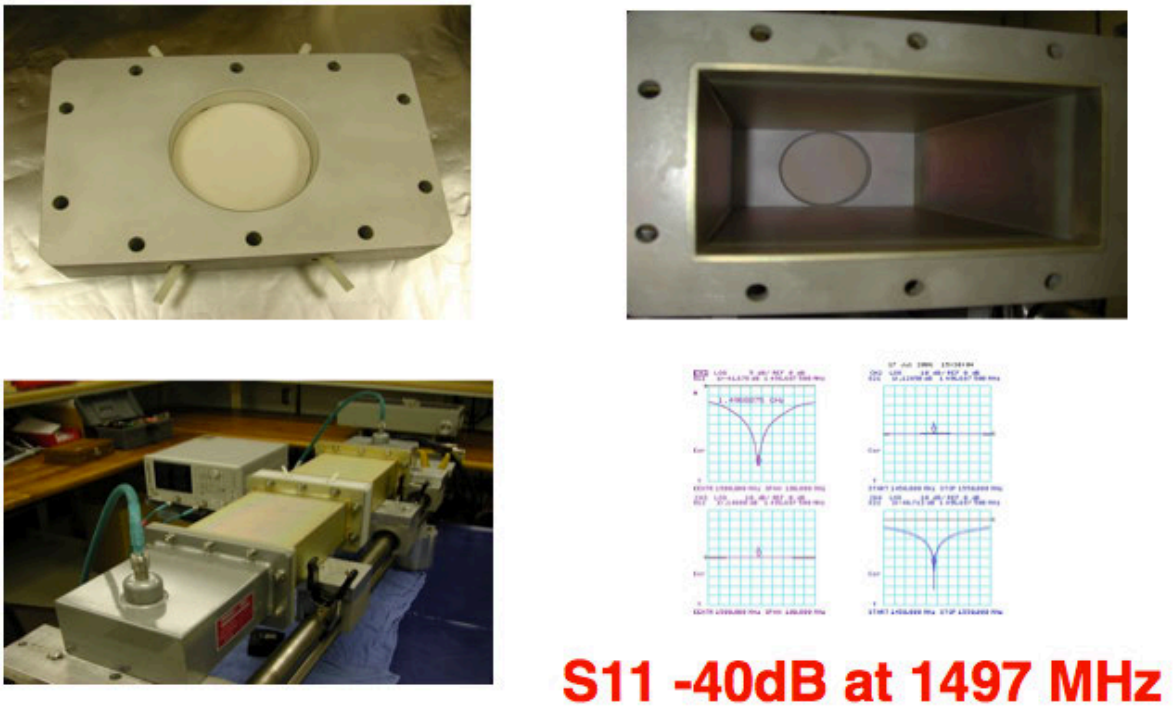

Figure 2: RF cold test measurements of the 50 kW CW RF window.

Out of the two options for coupling power into the gun, equatorial coupling or on-axis coupling, we still favor using on-axis coupling. This decision is largely driven by thermal/mechanical considerations in the design. Equatorial coupling requires either additional port(s), resulting in less material and hence higher heat loads around the equator, or the use of port(s) formally dedicated for vacuum pumping. The ability to operate at ultra high vacuum ($<10^{-9}$ Torr) is key to the operation of photocathode guns, and particularly important for CW operation which usually calls for the use of semiconductor cathodes, in which case vacuums $<10^{-10}$ Torr are required. Therefor it is very desirable to maintain sufficient pumping capability.

A preliminary design for a door-knob coupler was developed by R. Rimmer (JLab). This waveguide to coax adapter provides on axis coupling with variable beta (See Figure 3).

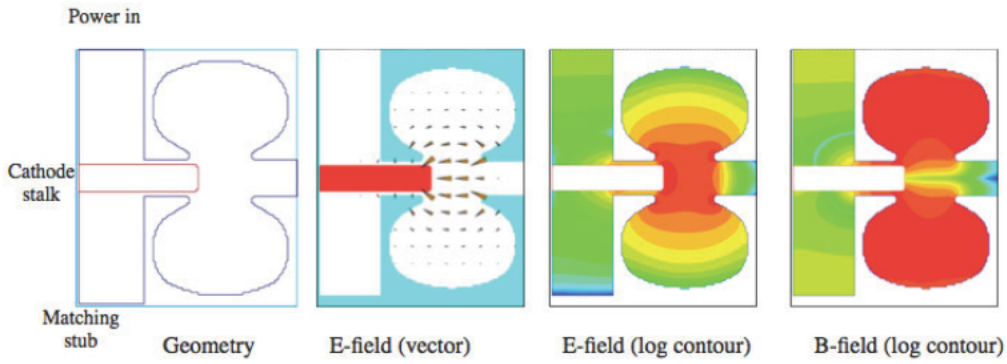

Figure 3: 2D RF simulations of waveguide to coax adapter.

3D RF simulations of the waveguide to coax coupler were carried out at RadiaBeam (See Figure 4). The WR650 waveguide is connected to the coax through a door knob type coupler. The geometric dimensions of the transition and the depth of the inner conductor will be optimized in order to obtain the desired coupling coefficient.

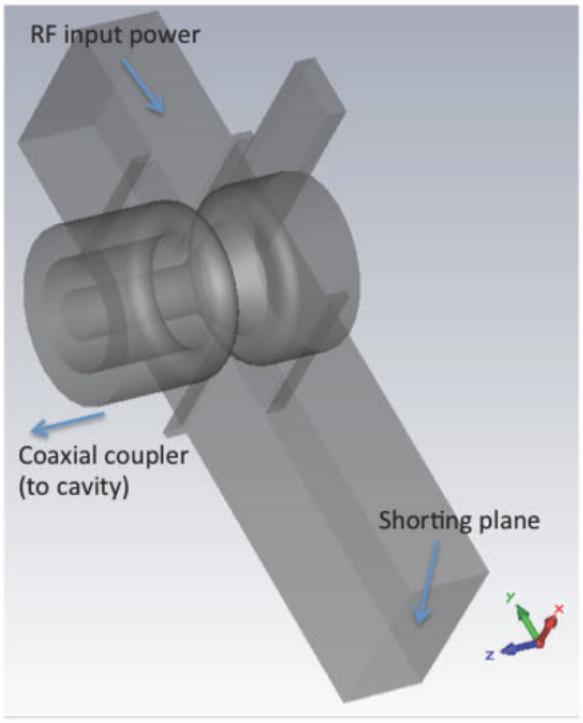

Figure 4: 3D simulations of waveguide to coax coupler.

B.2.2. Structure thermal-mechanical design

Following the completion of the RF design, thermal-mechanical simulations where carried out to optimize the cavity's cooling circuit. Figure 5 shows the cooling channel geometry simulated, along with typical flow parameters used.

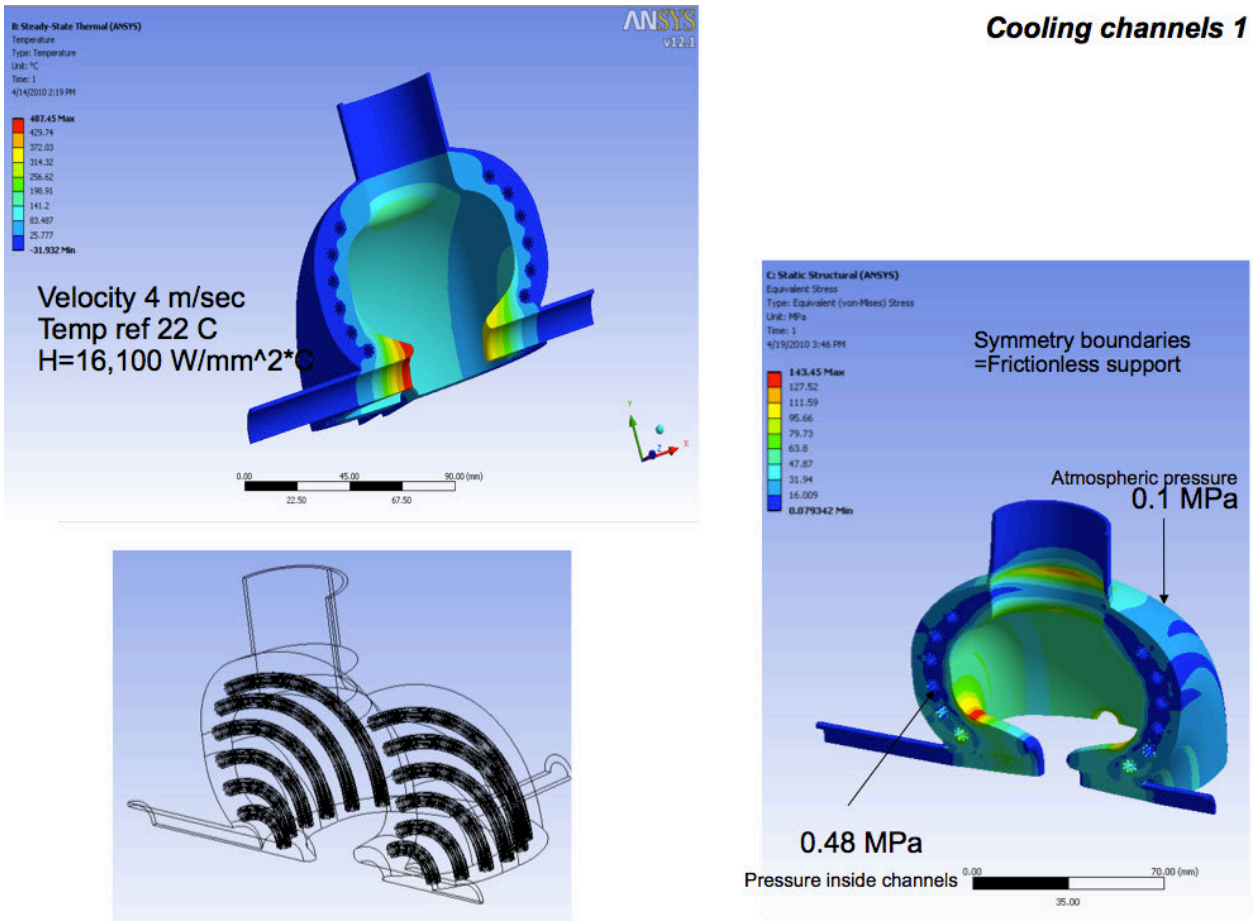

Figure 5: ANSYS simulations of the CW cavity.

Based on the optimized cooling circuit geometry, a CAD model was generated with realistic circuit elements (See Figure 6). We note here that the cooling geometry developed fully exploited the advantages of additive manufacturing, in particular the ability to realize imbedded conformal channels with complex geometries. Such a geometry has been realized for the first time in pure copper, and is reported in greater deal in later sections of this report.

The final CAD model (i.e. the model with final RF dimensions) was modified for EBM fabrication. This step is required due mainly to the relatively rough finish of the as-EBM part; secondary machining of the RF surfaces is necessary. Therefore the EBM model has an additional 5mm of material on all RF surfaces (and brazing surfaces), and it also includes the

addition of a sacrificial support structure to better maintain the overhanging geometry of the gun cavity. Figure 7 shows a comparison of the final CAD geometry and the EBM input geometry.

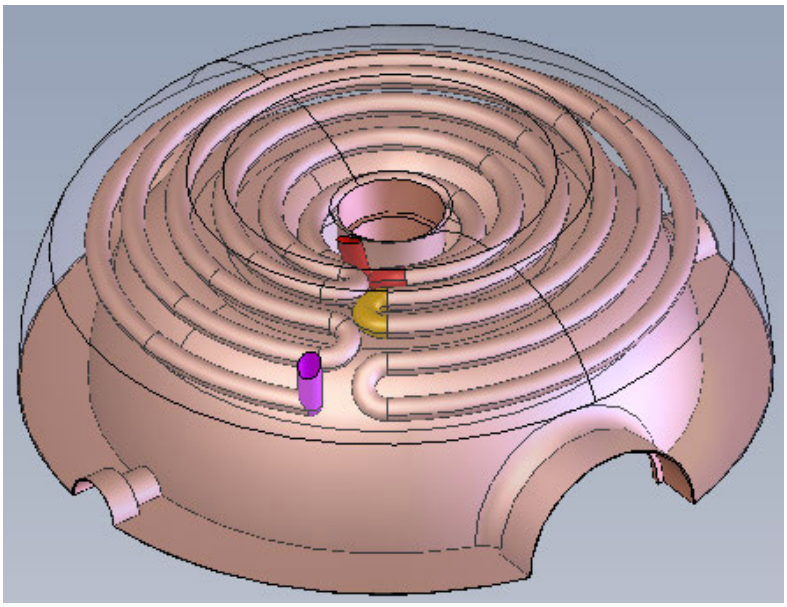

Figure 6: CAD rendering showing the 3D conformal nature and fully integrated cooling circuit design of the CW.

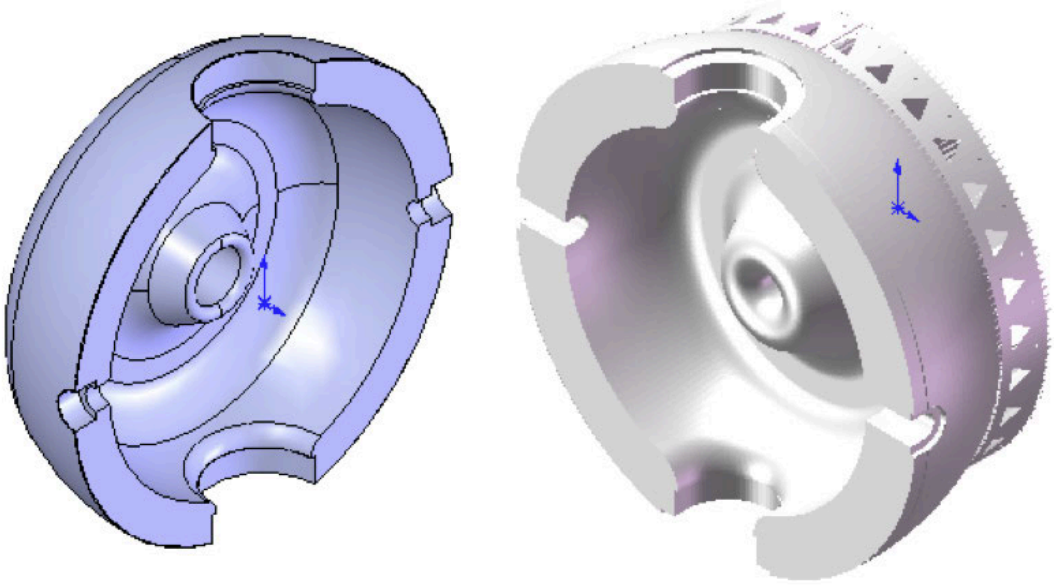

Figure 7: CAD rendering of the final design (left), and the EBM modified design (right).

B.3. ˚*EBM process optimization and fabrication*

B.3.1. EBM process optimization

The first task in the EBM process optimization is the optimization of the feedstock powder. This task was successfully carried out in the first year of the Phase II.

After thoroughly validating the vendor's copper powder, a number of parts were EBMed to verify material properties, and RF performance. Figure 8 (Left) shows a 3D micrograph construction from an EBM coupon, and (Right) an optical micrograph at high magnification of the same copper coupon. The relatively equiaxed grain structure containing annealing twins found is the EBM sample is comparable to that found in wrought C10100 annealed copper. However, this is not the typical (default) microstructure obtain in the EBM process; it took extensive EBM parameter development to achieve such an equiaxed state.

The pure copper EBM process parameters (aka "themes") developed in the course of this Phase II study at UTEP, and a sister study at NCSU, have attracted significant interest from the additive manufacturing community. Oak Ridge National Laboratory's Manufacturing Demonstration Facility (ORNL-MDF), which utilizes the same EBM technology, contacted RadiaBeam Technologies and collaborators UTEP and NCSU, and expressed interested in using the copper themes to produce high efficiency heat exchangers in applications such as nuclear submarine propulsion systems [15].

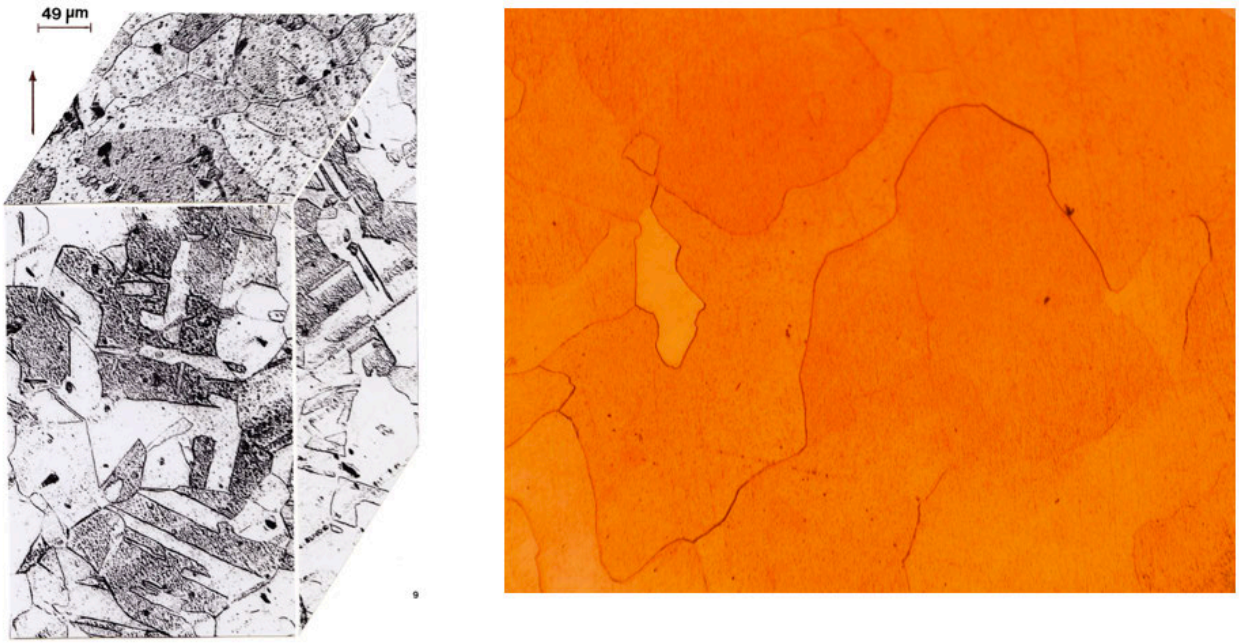

Figure 8: 3D construction of an EBM copper sample using the high purity copper powder (Left). Optical micrograph of EBM copper sample.

Larger samples were also EBMed, including a cooling channel test block, and several cathode blanks suitable for testing under high power RF (See Figure 9, and Figure 10).

A cooling channel test block, measuring 3"x3"x2" and featuring internal cooling channels of varying diameters and paths lengths, was EBM to verify minimum curve radii and diameters are consistent with those used in the SFF CW Gun design. Figure 9 shows the cooling channel test block.

Figure 9: 3D CAD model of the cooling channel test block (CCTB) showing internal cooling channel geometry (Left), and photographs of the sectioned EBMed CCTB showing cooling channels of 1.5mm, 4mm, and 7mm in diameter.

In channels with diameters of 1.5mm the copper powder sintered to the point where it was not possible to clear in all but cases of straight paths. Channels with larger diameters (4 and 7 mm) where easily cleared even with bend radii as small as 7.5 mm. These results more than satisfy the minimum cooling channel diameters (5mm) and bend radii (>10mm) found in the gun cooling design.

In order to verify the ultimate RF performance of the EBM copper, a copper cathode, suitable for testing in the UCLA 1.6 cell photoinjector, was also EBMed. Figure 10 shows the cathode in the as EBM condition, after final machining, and being installed in the Pegasus photoinjector. No other heat treatment was carried out on the EBM cathode prior to final machining.

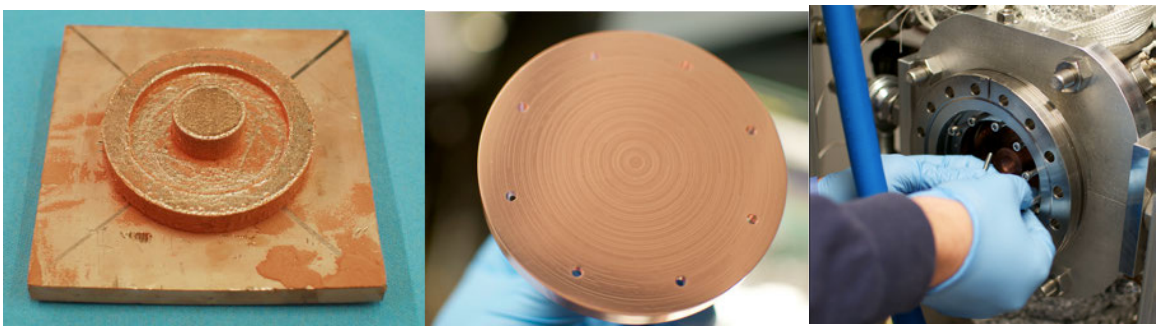

Figure 10: Photograph of the cathode blank in the as EBM condition (Left), and after final machining, and installation in the UCLA Pegasus 1.6 cell Photoinjector.

High power RF testing of the EBM cathode was successfully carried out, with the EBM copper cathode performing as well as other cathodes conventionally machined from wrought OFE copper material. Stable operation with 70 MV/m peak (limited by RF system) fields on the cathode was achieved after 2 hours of RF conditioning. Photoelectron beam with energy of 3.3 MeV and charge of 60 pC was measured, along with a cathode quantum efficiency of ~$2x10^{-5}$. These numbers are entirely consistent with conventional OFE copper cathodes measured in the past at Pegasus, given the operating gradient. It's worth noting that the Pegasus 1.6 cell photoinjector continues to run with the EBM cathode to this date, and we will have the opportunity to make a full QE map, as well as evaluate the long term performance of the EBM material.

Table 1: Summary of measured copper EBMed material properties in comparison to the wrought material (right), and comparison of the Arcam developed titanium alloy (left).

	EBM Ti6AL4V [16]	**Wrought Ti6Al4V (ASTM F1472)**	**EBM Copper**	**Wrought C10100 Copper**
Density	>99.9%		8.84 g/cm^3	8.90 g/cm^3
Electrical Conductivity @ 20˚ C	_	_	97 % IACS	102 %IACS
RRR	_	_	Planed or in progress	_
Thermal Conductivity	_	_	390 W/m*K	391 W/m*K
YS (Rp 0.2)	950 MPa	860 MPa	76 MPa	69 MPa
UTS (Rm)	1020 MPa	930 MPa	172 MPa	220 MPa
Elongation	14 %	> 10%	Planed or in progress	_
Reduction Area	40%	> 25%	Planed or in progress	_
Fatigue strength @ 600 MPa	>10M cycles	_	Planed or in progress	_

Table 1 summarizes the measured copper EBMed material properties, and compares them to wrought C10100 copper; a comparison of the ARCAM developed titanium alloy is also shown for reference. We note that Arcam, the manufacturer of the EBM system used in this study, took nearly 10 years to fully optimized its proprietary Ti alloy powder and associated EBM themes.

We think it is remarkable that pure copper EBM parameters, developed for the first time by RadiaBeam and collaborators funded under DOE SBIR/STTR grants as well as RadiaBeam internal R&D, have been nearly optimized in less than a quarter of that time.

Although we have successfully developed and demonstrated EBM additive manufactured copper material and RF performance on smaller sample geometries in the course of this Phase II study, were did not fully realize (or test under high power RF) a complete L-band CW cavity as originally proposed. The reasons for this are discussed in the next section.

B.4. *Structure testing, and what was learned*

RF cold and hot tests planned for in Phase II were not completed as planned within the Phase II timeframe. Secondary processing, including machining and brazing test were completed. Below we report on the EBM fabrication challenges encountered.

The Phase II schedule called for a total of 12 weeks to fabricate the prototype cavities. We envisioned fabricating multiple cavities to allow for secondary processing trials and possible losses due to machining or brazing, as well as high power testing at JLab. Over a period of six months, dozens of EBM runs were carried out. A typical (half) cavity build time is approximately 12 hours (as calculated by the EBM machine). In the entire course of fabrication all but one (half) cavity suffered from a catastrophic build-failure before the geometry was completed. Figure 11 shows a picture of the only successful cavity build.

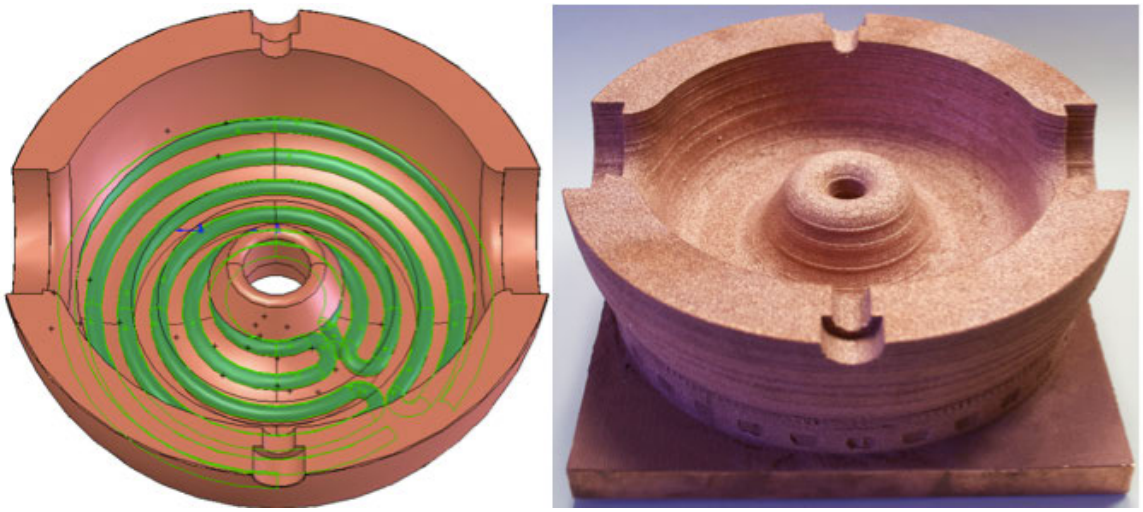

Figure 11: (Left) CAD rendering of an NCRF L-band cavity with internal cooling channels, and (Right) the realized as-EBM cavity. The EBM cavity is made with an extra 5 mm of material on the RF surfaces in preparation for post processing (machining & polishing).

The initial EBM runs utilized the recently developed pure copper EBM themes previously shown to yield excellent material results albeit in smaller parts. However, these themes resulted in curling of the copper layers near the OD of the cavity. Once a layer begins to curl, succeeding layers quickly start to delaminate, and the entire build is ruined. This behavior would occur

several hours into the build. Custom, geometry specific themes were developed to overcome this problem.

The need for custom, geometry specific, themes in the Arcam EBM process was not a complete surprise. Previous studies by UTEP and others utilizing titanium and nickel based super alloys had indicated the need for fine tuning of process themes for specific geometries. However, the EBMing of pure copper posed a problem not encountered with previous materials.

Early runs resulted in severe delamination thought to be cause by a significant thermal gradient within each layer. By the time the beam finished rastering a layer; the previously melted areas had cooled and contracted, subsequently separating the layer(s). The high thermal conductivity of the copper powder (particularly after sintering/melting) was suspected to be the cause. To counteract the high thermal loss, the copper substrate was insulated by various means to slow heat transfer of the powder to the build platform and chamber. The start temperature of the substrate and the powder surface temperature were also increased. Utilizing this set of new themes complete interlayer fusion was achieved, however microstructural examination showed a relatively porous parts, with columnar grain growth (See Figure 12). Over melting (or over sintering) of the powder also made powder recovery difficult or impossible, resulting in the loss of a significant amount of powder.

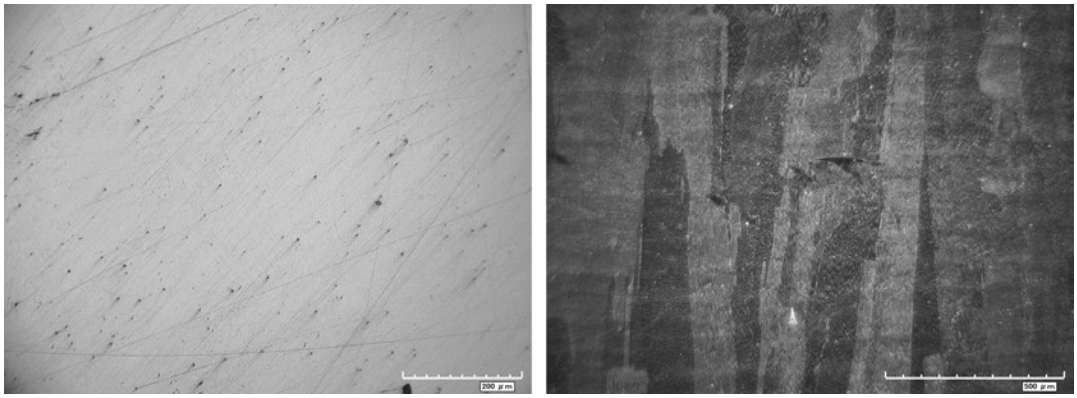

Figure 12: Micrographs showing the polished surface of a copper sample from experiment showing porosity (left) with 200µm scale bar and the etched surface (right) showing interlayer grain growth 500µm scale.

The extremely small process parameter window of UTEPs EBM machine needed to fabricate the CW gun geometry, and the limited time and powder allocated for the study, resulted in the failure to produce a complete EBM cavity suitable for RF power testing.

One possible solution to the problems encountered in the Phase II fabrication of the full scale photoinjector is increasing the size of the Arcam EBM build platform. The EBM A2 system used at UTEP has a build diameter of 200 mm. Using titanium powder, parts up to that (200 mm) diameter have been successfully fabricated. However, the higher thermal conductivity of copper reduces the effective build diameter to <150mm. Figure 13 shows the relative size of the CW cavity and build diameter. Unfortunately, the design, fabrication, implementation of a new EBM build platform/chamber was outside the scope of this Phase II.

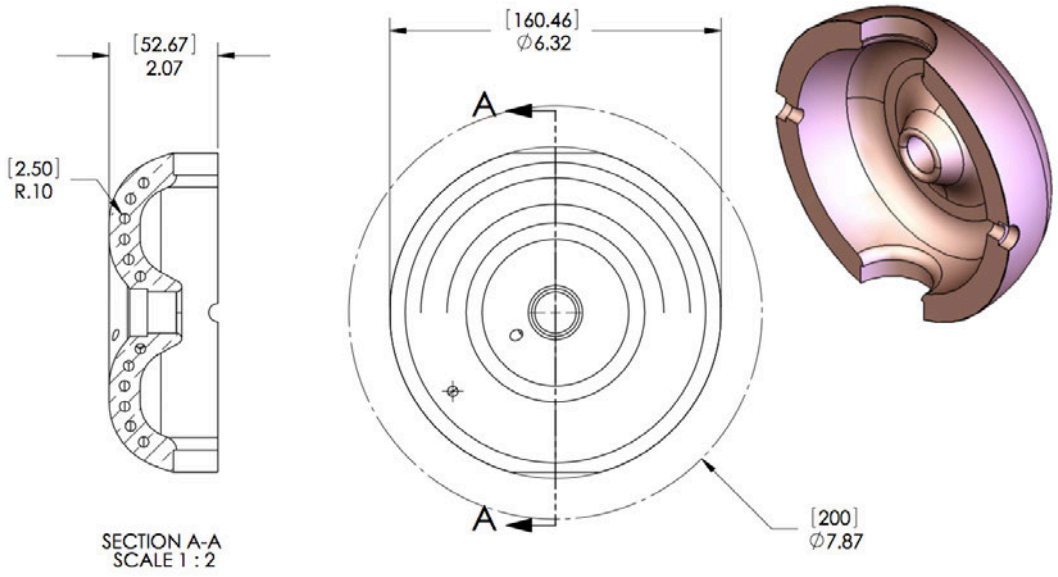

Figure 13: CAD drawing of the CW half cavity showing its geometry and relative dimension to the EBM build volume (200 mm).

B.5. *Conclusions*

B.5.1. Present Status

RadiaBeam Technologies in collaboration with the University of Texas at El Paso has developed pure copper process parameters for the Arcam electron beam melting (EBM) additive manufacturing (AM) technology. Material and RF testing of small EBM components parts have been successfully carried out, yielding results comparable to that of wrought C10100 copper. However, a full scale L-band CW photoinjector cavity was not successfully fabricated (or tested) and planned.

RadiaBeam has identified a number of EBM hardware upgrades that could make the fabrication of the L-band CW photoinjector possible. RadiaBeam is currently engaged in a new collaboration with UTEP, for the development of niobium RF components, that will make hardware upgrades to the EBM platform.

B.5.2. Commercialization

Results from this Phase II study have been published in referred journals [17] and presented in conference proceedings [18]. As a result considerable interest has been expressed by the growing EBM additive manufacturing community.

As previously mentioned in this report, there is significant interest in the copper EBM process themes from ORNL. ORNL is interested in use the copper themes for the development of heat exchanges in nuclear power generation.

RadiaBeam continuous to actively develop the EBM technology under new SBIR/STTR funding.

B.5.3. Acknowledgment

The collaborators instrumental to the success of the project include: Frank Medina (formally UTEP, now ORNL-ARCAM), Diana Ramirez (UTEP), Lawrence Murr (UTEP), Edwin Martinez (UTEP), Ryan Wicker (UTEP), Tim Horn (NCSU), Ola Harrisson (NCSU), Robert Rimmer (JLab), W. Clemens (JLab), J. Henry (JLab), Frank Marhauser (JLab), A. Wu (JLab), and X.Zhao (JLab).

C. Bibliography

1 Linac Coherent Light Source (LCLS) Conceptual Design Report, SLAC-R-593, Chapter 1, 9 (2002).

2 I. V. Pogorelsky, et al., Phys. Rev. ST Accel. Beams 3, 090702 (2000).

3 A. M. M. Todd, "State-of-the art electron guns and injector designs," 32nd ICFA Advanced Beam Dynamics Workshop on Energy Recovery Linacs, Newport News, VA, USA, March 19, 2005.

4 J. Corlett, et al., Proc. PAC07, Albuquerque, NM, 2007, p. 1167.

5 I. Ben-Zvi, I.V.Bazarov, NIM A 557, 337 (2006).

6 Summary of working group on guns and injectors, 41st Advanced ICFA Beam Dynamics Workshop on Energy Recovery Linacs, Daresbury Laboratory, UK, May 21-25, 2007.

7 International Linear Collider Technical Review Committee Second Report, SLAC Tech. Pub. Dept., Chapter 2, 15 (2003)

8 TRex-FINDER. C.P.J. Barty, UCRL-TR-210425 (LLNL, 2005)

9 S. S. Kurenoy, D.C. Nguyen et al., "Normal-Conducting High Current RF Photoinjector for High Power CW FEL", Proceedings of Particle Accelerator Conference, 2005.

10 D. Dowell et. al., "First Operation of a Photocathode Radia Frequency Gun Injector at High Duty Factor", Appl. Phys. Lett., Vol. 63, No. 15, 11 October 1993.

11 A. Zholents, R. Rimmer, O. Walter, W. Wan, M. Zolotorev, "FEL Design for Power Beaming", Free-Electron Laser Challenges II, Proceddings of SPIE, Vol. 3614, p.72, (1999).

12 L.E. Murr et al., J. Mech. Behav. Biomed. Mater., Vol. 2, Iss. 1, Jan. 2009, p.20-32.

13 D. Cormier et al., Rapid Prototyping Journal, Vol. 10, No. 1, 2003, p.35-41.

14 R. Akre, et al., Phys. Rev. ST Accel Beams, 11, 030703 (2008)

15 Private communications with Dr. Ryan Dehoff (ORNL), F. Medina (formally UTEP, now ORNL-ARCAM) and Mr. Tim Horn (NCSU).

16 Arcam T64 Material Data Sheet, (http://www.arcam.com/CommonResources/Files/www.arcam.com/Documents/EBM%20Materials/Arcam-Ti6Al4V-Titanium-Alloy.pdf)

17 D.A. Ramirez et. al., Acta Materialia, Vol. 59, Issue 10, June 2011, pp. 4088-4099.

18 P. Frigola et. al., "Development of a CW NCRF Photoinjector using Solid Proceedings of IPAC'10, Kyoto, Japan (2010).